



## Preparation and Dielectric Properties of Polyaniline-Coated Magnetite Nanocomposites

H.K. ABDULKADIR<sup>1D</sup>

Department of Chemical & Petrochemical Engineering, College of Engineering, University of Anbar, Ramadi, Iraq

\*Corresponding author: Tel: +964 7824519098; E-mail: habdulkadir56@uoanbar.edu.iq

Received: 23 July 2019;

Accepted: 28 October 2019;

Published online: 30 December 2019;

AJC-19731

The conductive polymers such as polyaniline (PANI) exhibit considerable electrical conductive properties. The coating of PANI with magnetic ( $\text{Fe}_3\text{O}_4$ ) nanoparticles formed composites ( $\text{PANI}/\text{Fe}_3\text{O}_4$ ) with required dielectric properties. The morphology result study of  $\text{PANI}/\text{Fe}_3\text{O}_4$  by field emission scanning electron microscope (FESEM) indicate the presence of PANI with tubes like structure containing different wt % of  $\text{Fe}_3\text{O}_4$  nanoparticles (5, 15, 25 wt %). The structural pattern investigated by XRD revealed the presence of  $\text{Fe}_3\text{O}_4$  nanoparticles at  $2\theta = 35.58^\circ$ , while the amorphous structure indicates the presence of PANI matrix. However, the chemical bonding analysis using FTIR shows chemical conjugation of bonds at 3336, 3300 and 3277  $\text{cm}^{-1}$  due to presence of NH group in PANI and OH group in  $\text{Fe}_3\text{O}_4$  nanoparticles, while presence of 504 and 526  $\text{cm}^{-1}$  suggesting that  $\text{Fe}_3\text{O}_4$  nanoparticles are present in the composites materials. The dielectric properties study by 4-point probe and VSM shows that PANI and  $\text{PANI}/\text{Fe}_3\text{O}_4$  nanocomposites exhibit good electrical properties (1.55 to 1.35 S/cm) which are decreasing with increase of  $\text{Fe}_3\text{O}_4$  nanoparticles, may be resulting due to insulating behaviour of the magnetic nanoparticles, while the magnetic properties of  $\text{PANI}/\text{Fe}_3\text{O}_4$  nanocomposites indicate super paramagnetic properties with saturation magnetization of (59.4, 5.96, 11.94 and 15.43 emu/g).

**Keywords:** Polyaniline,  $\text{Fe}_3\text{O}_4$ , Conductivity, Magnetic properties.

### INTRODUCTION

In the last few decades, polymer nanocomposites have been an extensive area of research, due to their promising application in the field of science and engineering [1]. The conducting polymers such as polyaniline (PANI) has emerged as promising candidate for many applications. The PANI was found to be the most outstanding conducting polymer in the recent time with extraordinary electrical conductive properties, its higher stability and environment friendly make it suitable for chemical sensors and biosensing applications [2]. PANI was found to be suitable for covalent bond of the molecules due to its active idealized oxidative form, that gives PANI ability to form bond with other inorganic nanoparticles such as nickel, cobalt and iron oxide nanoparticles [3]. Electromagnetic nanocomposites are promising materials for several applications including electromagnetic radiation shielding, microwave absorption, sensors and biosensors [4,5]. Recently, electromagnetic nanocomposites has been prepared using highly magnetic nanoparticles like nickel and cobalt for micro-

wave absorption and electromagnetic shielding application, but these nanoparticles are toxic and therefore cannot be used for biomedical applications. Based on these findings our attention has move to iron oxide nanoparticles, which were found to have three different polymorphic forms that include hematite ( $\alpha\text{-Fe}_2\text{O}_3$ ), maghemate ( $\gamma\text{-Fe}_2\text{O}_3$ ) and magnetite ( $\text{Fe}_3\text{O}_4$ ). Among them  $\text{Fe}_3\text{O}_4$  nanoparticle is the most essentials candidate due to its higher saturation magnetization and low resistivity at microwave frequency, these make it suitable for many application such as magnetic recorder, ferrofluid, magnetic imaging resonance and soft magnetic materials [6,7]. Blending magnetic nanoparticles with conducting polymers has become a promising and most considerable approach to achieve desired modulated electromagnetic functional nanomaterials [8,9]. Tongyan *et al.* [10] published about the specific composites hybrid with suitable dielectric properties using  $\text{Fe}_x\text{O}_y$  (24 nm) blended with PANI, the composites results exhibit low electric and magnetic properties,  $10^{-5}$  to  $10^{-1}$   $\text{Scm}^{-1}$  and coercive force of  $H_c = 0$ , respectively [11,12]. Many papers were reported addressing the structure and properties of the composites

materials, which are usually dependent on the preparation method, shape, size of the particle and polymer-nanoparticles interaction. Many researchers and industries developed different methods to prepare composites with required dielectric properties [13,14], but until now precipitate magnetic nanoparticles were normally prepared in advance and then polymerized together with suitable polymer to achieve desired dielectric properties [15].

In the past few decades, conductive polyaniline (PANI) certain quantity of magnetic nanoparticles such as  $\text{Fe}_3\text{O}_4$  nanoparticles are investigated because of their suitable magnetic properties, flexibility, high environmental stability, easy preparative method and efficient biocompatibility [16]. They have high ability to be used in the biomedical industries, such as for targeted drug delivery, hyperthermia treatment, cell separation, magnetic resonance imaging, sensitivity and selectivity and the separation of biochemical products [17,18]. Furthermore, composites of PANI/ $\text{Fe}_3\text{O}_4$  serve for many applications that include, aptasensors, chips, a field-effect transistor (FET), DNA and those has display high-performing sensing properties toward target biological species [19,20]. The entire problem associated with preparation of PANI/ $\text{Fe}_3\text{O}_4$  nanocomposites as well as their properties were carefully controlled through the synthesis [21,22]. Until nowadays, where PANI nanotubes contain different content of  $\text{Fe}_3\text{O}_4$  nanoparticles have been studied without any surfactant [23] and the product obtained by this study exhibit ferromagnetic behaviour, with high saturation magnetism [24] for different application such optoelectronic, microwave absorption and biomedical application. Sol-gel techniques are employed to synthesize PANI/ $\text{Fe}_3\text{O}_4$  nanocomposites. The report indicated that the composites were agglomerated during the process gel became xerogel due to change in temperature which confirms the composites exhibit super paramagnetic properties by having saturation magnetization of 86 emu/g for pure  $\text{Fe}_3\text{O}_4$  nanoparticles which decrease with variation nanoparticles in the composites [25]. PPY/ $\text{Fe}_3\text{O}_4$  nanocomposites are synthesized through ultrasonic irradiation method and the result showed the concentration of doping as primary factor which varies the conductivities of PANI nanocomposites thereby, used for the development of electrochemical sensor [26]. Furthermore, different synthesis method are used to synthesize PANI/ $\text{Fe}_3\text{O}_4$  nanocomposites. The analysis result shows the variation in shape, size and the magnetite properties of the composites, while the morphology and agglomerated nature of the composites are due to homogeneity and continuous size distribution of the particles [27]. The morphological results of PANI/ $\text{Fe}_3\text{O}_4$  nanocomposites prepared *via* chemical co-precipitation method showed that composites were agglomerated with spherical shape and size [28].

In this work, the magnetite ( $\text{Fe}_3\text{O}_4$ ) nanoparticles was synthesized using chemical co-precipitation method. The precipitate was then polymerized with aniline monomer through assisted sol-gel method to obtain the solution of PANI/ $\text{Fe}_3\text{O}_4$  nanocomposites with excellent dielectric properties. The dielectric properties of the composites were studied using vibrating sample magnetometer (VSM) and standard 4-point probe apparatus while the morphology, structural pattern, chemical bonding analysis were investigated using field emission scanning electron

microscope (FESEM), X-ray diffraction (XRD) and Fourier transformation infrared spectra, respectively.

## EXPERIMENTAL

Aniline was purchased from the Sigma Aldrich Chemical industries and stored at temperature below 0 °C. The chemicals were used as received without further purification such as  $\text{FeCl}_2 \cdot 4\text{H}_2\text{O}$ ,  $\text{FeCl}_3 \cdot 6\text{H}_2\text{O}$ , ammonium solution, hydrochloric acid and ammonium persulfate (APS) and are used in the preparation of PANI,  $\text{Fe}_3\text{O}_4$  and PANI/ $\text{Fe}_3\text{O}_4$  nanocomposites.

**$\text{Fe}_3\text{O}_4$  nanoparticles preparation:** The chemical co-precipitation method is one of the most simplest chemical synthesis methods which is used to prepare  $\text{Fe}_3\text{O}_4$  nanoparticles as described by Rajesh *et al.* [29]: 4.35 g of  $\text{FeCl}_3 \cdot 6\text{H}_2\text{O}$  and 0.83 g of  $\text{FeCl}_2 \cdot 4\text{H}_2\text{O}$  were dispersed in 100 mL of distilled water under magnet for 1 h at 60 °C. Subsequently followed by addition of 5 mL of ammonia solution in dropwise into the mixture, the reaction was kept under magnetic stirrer for 0.5 h more at 70 °C. Finally the precipitate was allowed to cool down at room temperature and later was filtered, washed and dried in oven at 50 °C for 24 h.

**PANI/ $\text{Fe}_3\text{O}_4$  nanocomposites preparation:** The PANI/ $\text{Fe}_3\text{O}_4$  nanocomposites preparation was synthesized [30], 5, 15 and 25 wt % of the synthesized  $\text{Fe}_3\text{O}_4$  nanoparticles was dispersed in 10 mL of HCl and 2 mL of aniline monomer was then added into the mixture to obtained emulsion of aniline/ $\text{Fe}_3\text{O}_4$  sol. Separately, 0.81 g of ammonium persulfate dissolved in 10 mL of HCl and then added in the above reaction of aniline/ $\text{Fe}_3\text{O}_4$  solution to obtain stable dark green precipitate of PANI/ $\text{Fe}_3\text{O}_4$  nanocomposites. After washing with water and acetone the composites of PANI/ $\text{Fe}_3\text{O}_4$  was then dissolved in 5 mL of chloroform to obtain soluble solution of PANI/ $\text{Fe}_3\text{O}_4$  nanocomposites. In order to complete the process of gel formation, the above reaction was then dispersed into the solution of TEOS in deionized water.

**Characterization of composites:** The synthesized PANI/ $\text{Fe}_3\text{O}_4$  nanocomposites was investigated using special equipment as followed: in the first case, the dielectric properties of the composites was studied using standard four-point probe apparatus (Pro 4 Lucab Lab Mint SRC Malaysia) and vibrating sample magnetometer (VSM, analyzer, Lakeshore 7400 series model at room temperature), respectively, while the morphology, structural pattern and chemical bonding analysis were studied using field emission scanning electron microscope (FESEM, JEOL-2010) equipped with an energy dispersive X-ray spectroscopy EDS, OXFORD X-MAX, energy 200 premium UK, X-ray diffraction pattern (XRD, D8 FOCUS Bruker, Cu  $K\alpha$  line  $\lambda = 0.154056$  nm) and Fourier transformation infrared spectra (FTIR Nicolite 60 SXB), respectively.

## RESULTS AND DISCUSSION

**FESEM image of PANI/ $\text{Fe}_3\text{O}_4$  nanocomposites:** The morphology of the PANI and PANI/ $\text{Fe}_3\text{O}_4$  nanoparticles are investigated by FESEM and the results are shown in Fig. 1(a-b). The structure of PANI containing different content of  $\text{Fe}_3\text{O}_4$  nanoparticles (5, 10 and 25 wt %) was shown in the Fig. 1(b-d). It was observed that the entire sample of PANI/ $\text{Fe}_3\text{O}_4$  nano-

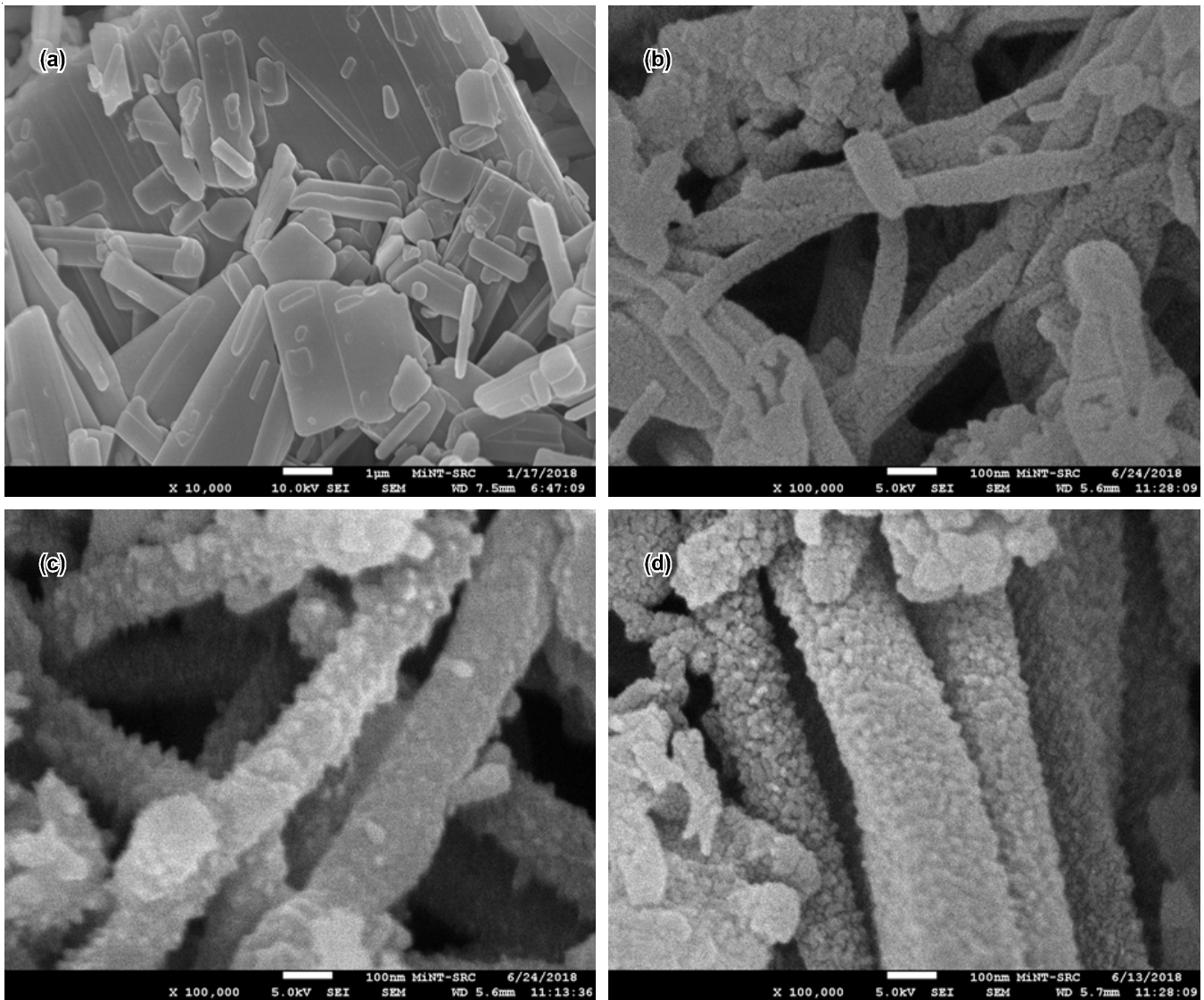


Fig. 1. FESEM images of (a) PANI (b) 5 wt.% of PANI/Fe<sub>3</sub>O<sub>4</sub> (c) 15 wt.% PANI/Fe<sub>3</sub>O<sub>4</sub> and (d) 25 wt.% PANI/Fe<sub>3</sub>O<sub>4</sub> nanocomposites

composites shows the morphology of nanofiber with diameter ranging from 60 to 100 nm, it was observed that the diameter of the PANI/Fe<sub>3</sub>O<sub>4</sub> nanocomposites was increasing over addition of Fe<sub>3</sub>O<sub>4</sub> nanoparticles as shown in Fig. 1 (b-d). In the process of polymerization of the composites particles showed that when the monomer of aniline was blended with Fe<sub>3</sub>O<sub>4</sub> nanoparticles then the monomer of aniline was able to absorb the nanoparticles through the process of electrostatic between the materials [31]. These lead to Fe<sub>3</sub>O<sub>4</sub> nanoparticles to be coated on the surface of PANI matrix [32], further secondary and primary growth was successfully been prevented which normally arise during polymerization of the composites materials, as result of Fe<sub>3</sub>O<sub>4</sub> nanoparticles in the PANI can easily be oxidized [33].

**XRD result of PANI/Fe<sub>3</sub>O<sub>4</sub> nanocomposites:** The structural pattern of PANI/Fe<sub>3</sub>O<sub>4</sub> nanocomposites and PANI particles were studied using XRD and the result was plotted in Fig. 2. The crystalline peaks appear at  $2\theta = 11.23^\circ, 17.24^\circ, 21.01^\circ, 23.45^\circ, 27.30^\circ, 32.38^\circ, 35.58^\circ, 61.24^\circ, 62.74^\circ, 68.10^\circ$  and  $77.31^\circ$  are assigned to (011), (101), (201), (112), (110), (121), (311), (122), (411), (510) and (501) were due to the presence

of Fe<sub>3</sub>O<sub>4</sub> nanoparticles in the composites. The highest intense peak observed at  $2\theta = 35.58^\circ$  indicate the presence of Fe<sub>3</sub>O<sub>4</sub> nanoparticles, suggesting that this composite contain Fe<sub>3</sub>O<sub>4</sub> nanoparticles. The broad peak that was observed at  $2\theta = 20-30^\circ$  in the amorphous pattern of the of PANI particles prepared without Fe<sub>3</sub>O<sub>4</sub> nanoparticles clearly shows the amorphous structure of the sample. The peaks revealed in the PANI/Fe<sub>3</sub>O<sub>4</sub> nanocomposites are due to presence of Fe<sub>3</sub>O<sub>4</sub> nanoparticles in the composites, suggesting that blending of PANI with Fe<sub>3</sub>O<sub>4</sub> nanoparticles did not temper the crystalline structure of the Fe<sub>3</sub>O<sub>4</sub> nanoparticles [34]. The values of FWHM and d-spacing of such peaks are tabulated in Table-1. The crystal structures of the samples were determined by the powder X-ray diffraction technique, the crystalline sizes calculated are listed in Table-1. These results indicated the structure of materials is cubic and Fe<sub>3</sub>O<sub>4</sub> nanoparticles were obtained. A similar result was observed by Takai *et al.* [34] and Xiao *et al.* [35]. The authors observed diffraction patterns of samples exhibited an increase in the peak intensity and a decrease in the full width at half-maximum (FWHM) and crystallite size increases due to nanoparticles concentration.

TABLE-1  
STRUCTURAL PARAMETERS OF THE PREPARED PANI/Fe<sub>3</sub>O<sub>4</sub> NANOPARTICLES DIFFERENT CONTENT OF Fe<sub>3</sub>O<sub>4</sub> NANOPARTICLES

| Samples                                     | 2θ (°) | FWHM   | d-spacing (Å) | hkl | Crystalline size (Å) |
|---|--------|--------|---------------|-----|----------------------|
| PANI/Fe <sub>3</sub> O <sub>4</sub> 5 wt %  | 35.58  | 0.0149 | 2.346         | 311 | 26.40                |
| PANI/Fe <sub>3</sub> O <sub>4</sub> 15 wt % | 35.34  | 0.0723 | 3.84023       | 311 | 33.60                |
| PANI/Fe <sub>3</sub> O <sub>4</sub> 25 wt % | 35.56  | 0.1723 | 2.346         | 311 | 38.80                |

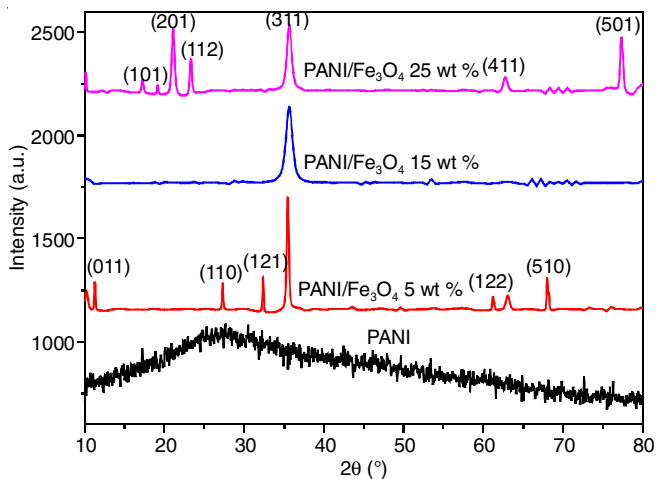


Fig. 2. XRD results of PANI and PANI/Fe<sub>3</sub>O<sub>4</sub> nanocomposites containing (5, 15, 25 wt.%) of Fe<sub>3</sub>O<sub>4</sub> nanoparticles

Furthermore, in the current research Scherer's equation:

$$D = \frac{\kappa\lambda}{\beta \cos \theta} \quad (1)$$

was used to estimated the size of the Fe<sub>3</sub>O<sub>4</sub> nanoparticles where  $\lambda = 0.1504$  nm is the wavelength of the X-ray, the shape factor denoted by  $\kappa = 0.89$ , the diameter of the crystal  $D$  and  $\theta$  is the Bragg angle and  $\beta$  is the Full width at half maximum (FWHM). Therefore, the crystalline peak appearing at  $2\theta = 35.57$  indicates the presence of Fe<sub>3</sub>O<sub>4</sub> nanoparticles and was used to calculate the size of the particles which was found to be 26.4, 33.6 and 38.8 nm with addition of Fe<sub>3</sub>O<sub>4</sub> nanoparticles [36].

**FTIR result of PANI/Fe<sub>3</sub>O<sub>4</sub> nanocomposites:** The chemical bonding structure of the PANI and PANI/Fe<sub>3</sub>O<sub>4</sub> nanocomposites was investigated using FT-IR spectra and the result is shown in the Fig. 3. The spectra of the pure PANI revealed a weak peak at  $3300\text{ cm}^{-1}$  which was due to presence of NH vibrating stretching that is usually found in the PANI particles. These regions provide absorption surface of hydrogen bond with water molecule. While, some peaks observed at  $1625\text{ cm}^{-1}$  and  $869\text{ cm}^{-1}$  was assigned to the vibration stretching of PANI matrix [37]. However, the structural peaks observed in the PANI/Fe<sub>3</sub>O<sub>4</sub> nanocomposites was measured and the study observed some weak bands at  $3336, 3300$  and  $3277\text{ cm}^{-1}$  are due to OH and NH of the Fe<sub>3</sub>O<sub>4</sub> nanoparticles and PANI particles that allowed hydrogen bond formation between the two particles. The peaks observed at  $1625, 1076$  and  $869\text{ cm}^{-1}$  which are assigned to C=C, C=N are due to vibrating mode of stretching quinonoid (NH- $\theta$ -NH) of the covalent bond [38]. The peaks at  $884$  and  $869\text{ cm}^{-1}$  were attributed to C-C, C-N vibrating stretching modes of benzenoid ring of covalent bond. Furthermore, presence of Fe<sub>3</sub>O<sub>4</sub> nanoparticles was detected by observing the peaks at  $504$  and  $526\text{ cm}^{-1}$ , these shifting of peaks was due to surface interaction of  $3d$  orbital of the ferrite particle with

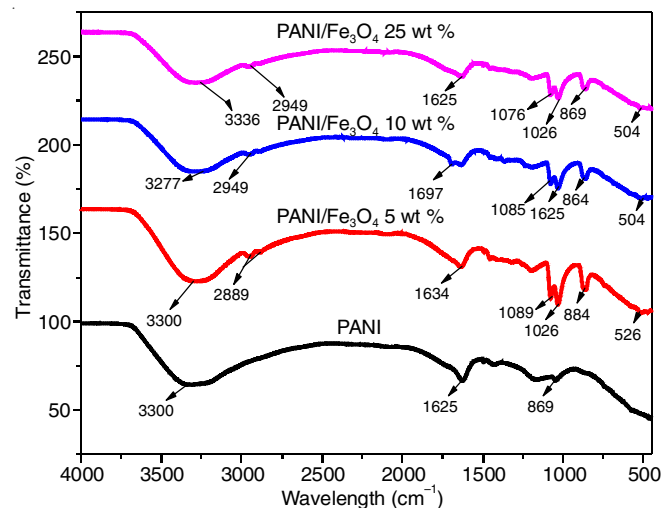


Fig. 3. FT-IR analysis of PANI and PANI/Fe<sub>3</sub>O<sub>4</sub> nanocomposites containing (5, 15, 25 wt.%) of Fe<sub>3</sub>O<sub>4</sub> nanoparticles

nitrogen atoms in the PANI which leads to the formation of coordinate bond between the particles [39,40]. The Fe<sub>3</sub>O<sub>4</sub> nanoparticles was coated on the PANI surface through the process of hydrogen bonding usually between O-H group of magnetite nanoparticles and N-H group of PANI particles, the bond of PANI and Fe<sub>3</sub>O<sub>4</sub> nanoparticles through hydroxyl group was strongly confirmed by the FITR analysis [41,42].

**Electrical conductivity result of PANI/Fe<sub>3</sub>O<sub>4</sub> nanocomposites:** The conductivity of PANI and PANI/Fe<sub>3</sub>O<sub>4</sub> nanocomposites was studied using standard 4-point probe apparatus and the result was plotted in the Fig. 4. The protonated PANI particles without Fe<sub>3</sub>O<sub>4</sub> nanoparticles was found to have higher conductive values of  $2.1 \times 10^1$  S/cm while, the electrical conductivity of the PANI/Fe<sub>3</sub>O<sub>4</sub> nanocomposites was found to decrease from 1.55 to 1.35 S/cm, the variation of the conductivity was probability due to insulating behaviour of the Fe<sub>3</sub>O<sub>4</sub> nanoparticles thereby lowering the conductivity of the composites materials [43]. Hence the conductivity was decreasing over addition of Fe<sub>3</sub>O<sub>4</sub> nanoparticles in the matrix. Furthermore, sol-gel assisted chemical polymerization of PANI particles with different content of Fe<sub>3</sub>O<sub>4</sub> nanoparticles shows good electrical conductivity of the composites particles. The highest observable electrical conductivity (1.55 S/cm) was found at 5 wt % content of Fe<sub>3</sub>O<sub>4</sub> nanoparticles, the movement of charge carriers in the polymers enhance the electrical conductivity through charge transfer between conductive electron in the PANI and  $3d$  orbital of ferrite particles, proving that there is higher inter-component interaction with the matrix during polymerization which is usually achieved through direct mixing [44].

**Magnetic analysis of PANI/Fe<sub>3</sub>O<sub>4</sub> nanocomposites:** The magnetic properties of the Fe<sub>3</sub>O<sub>4</sub> nanoparticles and PANI/Fe<sub>3</sub>O<sub>4</sub> nanocomposites was study using vibrating sample magnetometer (VSM) and Table-2 tabulates the result obtained after

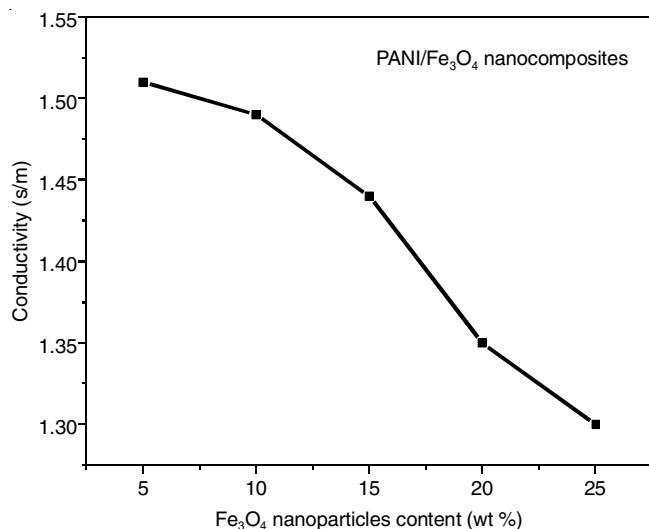


Fig. 4. Conductivity result of PANI and PANI/Fe<sub>3</sub>O<sub>4</sub> nanocomposites containing (5, 15 and 25 wt %) of Fe<sub>3</sub>O<sub>4</sub> nanoparticles

TABLE-2  
VARIATION OF SATURATION MAGNETIZATION  
WITH DIFFERENT CONTENT OF Fe<sub>3</sub>O<sub>4</sub> NANOPARTICLES  
IN PANI/Fe<sub>3</sub>O<sub>4</sub> NANOCOMPOSITES

| Content of Fe <sub>3</sub> O <sub>4</sub> (wt %) | Saturated magnetization (em/g) | Remnants magnetization (em/g) | Coercive force (emu/g) |
|--|--------------------------------|-------------------------------|------------------------|
| 100  | 59.4                           | 0                             | 0                      |
| 5  | 5.96                           | 0                             | 0                      |
| 15   | 11.94                          | 0                             | 0                      |
| 25   | 15.43                          | 0                             | 0                      |

studying the magnetic properties of the composites materials. In the process of analyzing the magnetic properties of Fe<sub>3</sub>O<sub>4</sub> and PANI/Fe<sub>3</sub>O<sub>4</sub> nanocomposites, the saturation magnetization ( $M_s$ ), coercive force ( $H_c$ ) and remnant magnetization ( $H_r$ ) were found to be from 5.96 emu/g to 15.43 emu/g for (5, 15 and 25 wt.%) Fe<sub>3</sub>O<sub>4</sub> nanoparticles content, indicating super paramagnetic performance of the PANI/Fe<sub>3</sub>O<sub>4</sub> nanocomposites, while pure Fe<sub>3</sub>O<sub>4</sub> nanoparticles had  $M_s$  value of 59.4 emu/g. Suggested that the saturation magnetization of the composites materials were quite lower than that of Fe<sub>3</sub>O<sub>4</sub> nanoparticles which is probably due to non-magnetic nature of the PANI matrix [45]. In general, interaction between the polymer matrix and  $d$ -orbital of ferrite particles was attributing to the electron with unpaired spins thereby varies the saturation magnetization of the composites materials [46]. In another case, due to higher transfer of charge carriers in PANI and Fe<sub>3</sub>O<sub>4</sub> nanoparticles usually hinder the magnetic performance of the composites. Hence, the variation of  $M_s$  of the composites was due to different interaction within the inter-phase of the PANI/Fe<sub>3</sub>O<sub>4</sub> nanocomposites materials [47].

## Conclusion

In summary, PANI nanostructure containing different content of Fe<sub>3</sub>O<sub>4</sub> nanoparticles was prepared *via* sol-gel technique. The polymerization process occurred by subsequent addition of APS/HCl into the emulsion of aniline/Fe<sub>3</sub>O<sub>4</sub>, while the gel was formed when PANI/Fe<sub>3</sub>O<sub>4</sub> nanocomposites were dispersed in TEOS solution. The analysis result shows that the dielectric properties of the composites materials study by VSM and 4-

point probe varies with variation of Fe<sub>3</sub>O<sub>4</sub> nanoparticles in the composites. The adjustable nature of electromagnetic properties of the composites can be used for many applications such microwave absorption, chemical sensors, optoelectronics and electromagnetic radiation. The XRD analysis revealed the presence of Fe<sub>3</sub>O<sub>4</sub> nanoparticles in the composites by shown the peaks at 35.58° which was further supported by FTIR analysis.

## ACKNOWLEDGEMENTS

The author gratefully acknowledges the Department of Chemical & Petrochemical Engineering, College of Engineering, University of Anbar, Ramadi, Iraq for their support and encouragement of this work, as well as Microelectronic and Nanotechnology-Shamsuddin Research Centre (Mint-SRC) Universiti Tun Hussein Onn Malaysia (UTHM) for technical assistance and characterization analysis.

## CONFLICT OF INTEREST

The authors declare that there is no conflict of interests regarding the publication of this article.

## REFERENCES

- W.L. Song, X.-T. Guan, L.-Z. Fan, Y.-B. Zhao, W.-Q. Cao, C.-Y. Wang and M.-S. Cao, *Carbon*, **100**, 109 (2016); <https://doi.org/10.1016/j.carbon.2016.01.002>.
- R. Qiang, Y. Du, Y. Wang, N. Wang, C. Tian, J. Ma, P. Xu and X. Han, *Carbon*, **98**, 599 (2016); <https://doi.org/10.1016/j.carbon.2015.11.054>.
- J. Qiu and T. Qiu, *Carbon*, **81**, 20 (2015); <https://doi.org/10.1016/j.carbon.2014.09.011>.
- W. Feng, Y. Wang, J. Chen, L. Wang, L. Guo, J. Ouyang, D. Jia and Y. Zhou, *Carbon*, **108**, 52 (2016); <https://doi.org/10.1016/j.carbon.2016.06.084>.
- K.S. Loh, Y.H. Lee, A. Musa, A.A. Salmah and I. Zamri, *Sensors*, **8**, 5775 (2008); <https://doi.org/10.3390/s8095775>.
- M.I. Kimpa, M.Z.H.B. Mayzan, F. Esa, J.A. Yabagi, M.M. Nmaya and M.A.B. Agam, *Int. J. Integr. Eng.*, **9**, 106 (2017); <https://doi.org/10.30880/ijie.2018.10.09.020>.
- K.G. Schell, E.C. Bucharsky, F. Lemke and M.J. Hoffmann, *Ionics*, **23**, 821 (2017); <https://doi.org/10.1007/s11581-016-1883-y>.
- H. Jaya, N.Z. Noriman, O.S. Dahham, N. Muhammad, N.A. Latip, A.K. Aini and K.M. Breesem, *IOP Conf. Series Mater. Sci. Eng.*, **454**, 012192 (2018); <https://doi.org/10.1088/1757-899X/454/1/012192>.
- J. Yin, X. Xia and X. Zhao, *Polym. Degrad. Stab.*, **97**, 2356 (2012); <https://doi.org/10.1016/j.polymdegradstab.2012.07.029>.
- P. Tongyan, L. Yang and W. Zhaoyang, *Polym. Degrad. Stab.*, **97**, 2331 (2012); <https://doi.org/10.1016/j.polymdegradstab.2012.07.032>.
- Z.J. Gu, J.R. Ye, W. Song and Q. Shen, *Mater. Lett.*, **121**, 12 (2014); <https://doi.org/10.1016/j.matlet.2014.01.133>.
- S. Sarmah and A. Kumar, *Bull. Mater. Sci.*, **36**, 31 (2013).
- S.Y. Patil, P.P. Mahulikar, S.J. Pawar and V.S. Zope, *Int. J. Adv. Sci. Tech. Res.*, **6**, 248 (2016).
- P. Jha, S. Rai, K.V. Ramanujachary, S.E. Lofland and A.K. Ganguli, *J. Solid State Chem.*, **177**, 2881 (2004); <https://doi.org/10.1016/j.jssc.2004.05.009>.
- M.F. Zawah, E.S.E. El-Shereefy and A.Y. Khudir, *Silicon*, **11**, 85 (2019); <https://doi.org/10.1007/s12633-018-9841-0>.
- J.H. Yu, S.V. Fridrikh and G.C. Rutledge, *Adv. Mater.*, **16**, 1562 (2004); <https://doi.org/10.1002/adma.200306644>.
- D.-L. Zhao, H.-L. Zhang, X.-W. Zeng, Q.-S. Xia, J.-T. Tang, *Biomed. Mater.*, **1**, 188 (2006); <https://doi.org/10.1088/1748-6041/1/4/002>.

18. S.P. Bhatnagar and R.E. Rosensweig, *J. Magn. Magnet. Mater.*, **149**, 198 (1995);  
[https://doi.org/10.1016/0304-8853\(95\)00378-9](https://doi.org/10.1016/0304-8853(95)00378-9).
19. Z.I. Takai, M.K. Mustafa and S. Asman, *Asian J. Chem.*, **30**, 2625 (2018);  
<https://doi.org/10.14233/ajchem.2018.21473>.
20. J. Mohammed, T.T. Carol T, H.Y. Hafeez, B.I. Adamu, Y.S. Wudil, Z.I. Takai, S.K. Godara and A.K. Srivastava, *J. Phys. Chem. Solids*, **126**, 85 (2019);  
<https://doi.org/10.1016/j.jpcs.2018.09.034>.
21. Z.I. Takai, R.S. Kaundal, M.K. Mustafa, S. Asman, A. Idris, Y. Shehu, J. Mohammad, M.G. Idris and M. Said, *Mater. Res.*, **22**, 1 (2018);  
<https://doi.org/10.1590/1980-5373-mr-2018-0404>.
22. M. Jamal, M.Z. Noh, S.A. Juboor, M.H.B. Wan and Z.I. Takai, *Int. J. Technol.*, **7**, 180 (2018);  
<https://doi.org/10.14419/ijet.v7i4.30.22107>.
23. J. Guo, X. Ye, W. Liu, Q. Wu, H. Shen and K. Shu, *Mater. Lett.*, **63**, 1326 (2009);  
<https://doi.org/10.1016/j.matlet.2009.02.068>.
24. W. Cheng, K. Tang, Y. Qi, J. Sheng and Z. Liu, *J. Mater. Chem.*, **20**, 1799 (2010);  
<https://doi.org/10.1039/b919164j>.
25. H.-W. Zhang, J. Li, H. Su, T.-C. Zhou, Y. Long and Z.-L. Zheng, *Chin. Phys. B*, **22**, 117504 (2013);  
<https://doi.org/10.1088/1674-1056/22/11/117504>.
26. M. Al-Ibrahim, O. Ambacher, S. Sensfuss and G. Gobsch, *Appl. Phys. Lett.*, **86**, 201120 (2005);  
<https://doi.org/10.1063/1.1929875>.
27. O. Chiscan, I. Dumitru, V. Tura, H. Chiriac and A. Stancu, *IEEE Trans. Magn.*, **47**, 4511 (2011);  
<https://doi.org/10.1109/TMAG.2011.215810>.
28. H.K. AbdulKadir, H. Jaya, N.Z. Noriman, O.S. Dahham, A.H. Mazelan, N.A. Latip and A.K. Aini, *IOP Conf. Series: Mater. Sci. Eng.*, **454**, 012191 (2018);  
<https://doi.org/10.1088/1757-899X/454/1/012191>.
29. Rajesh, T. Ahuja and D. Kumar, *Sens. Actuators B Chem.*, **136**, 275 (2009);  
<https://doi.org/10.1016/j.snb.2008.09.014>.
30. G. Salimbeygi, K. Nasouri, A.M. Shoushtari, R. Malek and F. Mazaheri, *Mater. Res.*, **8**, 455 (2013);  
<https://doi.org/10.1007/s13233-015-3102-5>.
31. K. Sujith, A.M. Asha, P. Anjali, N. Sivakumar, K.R.V. Subramanian, S.V. Nair and A. Balakrishnan, *Mater. Lett.*, **67**, 376 (2012);  
<https://doi.org/10.1016/j.matlet.2011.09.083>.
32. S. Vyas, S. Shivhare and A. Shukla, *Int. J. Res. Sci. Innov.*, **6**, 86 (2017).
33. Z.J. Gu, J.T. Wang, L.L. Li, L.F. Chen and Q. Shen, *Mater. Lett.*, **117**, 66 (2014);  
<https://doi.org/10.1016/j.matlet.2013.11.121>.
34. Z.I. Takai, M.K. Mustafa, S. Asman, K.A. Sekak, *Int. J. Nanoelectron. Mater.*, **12**, 2232 (2019).
35. S. Xiao, M. Shen, R. Guo, S. Wang and X. Shi, *J. Phys. Chem. C*, **113**, 18062 (2009);  
<https://doi.org/10.1021/jp905542g>.
36. A.J. Hadi, H. K. AbdulKadir, G.J. Hadi, K.B. Yusoh and S.F. Hasany, *Orient. J. Chem.*, **34**, 2 (2018);  
<https://doi.org/10.13005/ojc/340259>.
37. M.M. Lakouraj, E.N. Zare and P.N. Moghadam, *Adv. Polym. Technol.*, **33**, 1 (2014);  
<https://doi.org/10.1002/adv.21385>.
38. F. Fajaroh, H. Setyawan, W. Widiyastuti and S. Winardi, *Adv. Powder Technol.*, **23**, 328 (2012);  
<https://doi.org/10.1016/j.apt.2011.04.007>.
39. S.-N. Sun, C. Wei, Z.-Z. Zhu, Y.-L. Hou, S.S. Venkatraman and Z.-C. Xu, *Chin. Phys. B*, **23**, 037503 (2014);  
<https://doi.org/10.1088/1674-1056/23/3/037503>.
40. S.A. Wilson, R.P.J. Jourdain, Q. Zhang, R.A. Dorey, C.R. Bowen, M. Willander, Q.U. Wahab, M. Willander, S.M. Al-hilli, O. Nur, E. Quandt, C. Johansson, E. Pagounis, M. Kohl, J. Matovic, B. Samel, W. van der Wijngaart, E.W.H. Jager, D. Carlsson, Z. Djinnovic, M. Wegener, C. Moldovan, R. Iosub, E. Abad, M. Wendlandt, C. Rusu and K. Persson, *Mater. Sci. Eng. Rep.*, **56**, 1 (2007);  
<https://doi.org/10.1016/j.mser.2007.03.001>.
41. T. Sulistyarningsih, S. Juari Santosa, D. Siswanta and B. Rusdianso, *Int. J. Mater. Mech. Manuf.*, **5**, 16 (2017);  
<https://doi.org/10.18178/ijmmm.2017.5.1.280>.
42. M. Tajabadi and M.E. Khosroshahi, *Int. J. Chem. Eng. Appl.*, **3**, 3 (2012).
43. M.R. Patil, S.D. Khairnar and V.S. Shrivastava, *Appl. Nanosci.*, **6**, 495 (2016);  
<https://doi.org/10.1007/s13204-015-0465-z>.
44. P. Liu, W. Liu and Q. Xue, *Mater. Chem. Phys.*, **87**, 109 (2004);  
<https://doi.org/10.1016/j.matchemphys.2004.05.001>.
45. A. Fisli, R. Saridewi, S.H. Dewi and J. Gunlazuardi, *Adv. Mater. Res.*, **626**, 131 (2013);  
<https://doi.org/10.4028/www.scientific.net/AMR.626.131>.
46. M.A. Adamu, M.K. Mustafa and N.N.B. Ruslan, *ARPN J. Eng. Appl. Sci.*, **11**, 9725 (2016).
47. P.L. Hariyani, M. Faizal, R. Ridwan, M. Marsi and D. Setiabudidaya, *Int. J. Environ. Sci. Dev.*, **4**, 336 (2013);  
<https://doi.org/10.7763/IJESD.2013.V4.366>.